Research Article

Rain Attenuation Study over an 18 GHz Terrestrial Microwave Link in South Korea

Sujan Shrestha and Dong-You Choi ![ORCID]

Department of Information and Communications Engineering, Chosun University, Republic of Korea

Correspondence should be addressed to Dong-You Choi; dychoi@chosun.ac.kr

Absorption of microwave radio frequency signal by atmospheric rain and losses is prevalent at frequencies above 5 GHz. The functioning frequencies of 18 GHz are taken for the point-to-point microwave link system. This paper presents studies on rain attenuation at 18 GHz, which specifies minimum performance parameters for terrestrial fixed service digital radio communication equipment. It presents a 3.2 km experimental link at 18 GHz between Khumdang (Korea Telecom, KT station) and Icheon (National Radio Research Agency, RRA station). The received signal data for rain attenuation and the rain rate were collected at 10-second intervals over three year's periods from 2013 to 2015. During the observation period, rain rates of about 50 mm/hr and attenuation values of 33.38 dB and 21.88 dB occurred for 0.01% of the time for horizontal and vertical polarization. This paper highlights the discussion and comparison of ITU-R P.530-16, Moupfouma, Silva Mello, and Abdulrahman models and proposed an attenuation prediction approach where it presents the relationship between theoretical specific rain attenuation as specified by ITU-R P.838-3, $\gamma_{\%p}$, and effective specific rain attenuation, γ_{eff}. Additionally, it studies 1-minute rain rates derived from higher time integration of 5-minute, 10-minute, 20-minute, 30-minute, and 60-minute instances which are obtained from experimental 1-minute rainfall amounts that are maintained by the Korea Meteorological Administration (KMA). The effectiveness of the proposed approach is further analyzed for 38 and 75 GHz links which shows better prediction capability. Particularly, in an 18 GHz link under horizontal polarization, ITU-R P. 530-16 shows the relative error margin of 71%, 60%, and 38% where as 64%, 49%, and 42% were obtained under vertical polarization for 0.1%, 0.01%, and 0.001% of the time, respectively. The limitation of research lies on the experimental system that is set up in only one location; however, the preliminary results indicate the application of a suitable 1-minute rain attenuation model for a specific site. The method provides useful information for microwave engineers and researchers in making decisions over the choice of the most suitable rain attenuation prediction for terrestrial links operating in the South Korea region, particularly for lower frequency ranges.

1. Introduction

Above the 5 GHz operating frequency, liquid rain in the form of absorption and scattering becomes a serious contributor to transmission losses [1]. When designing a line-of-sight (LOS) microwave link or satellite link operating at a frequency above 5 GHz, the occurrence of rain along the transmission path is considered as a main impairment factor for microwave system degradation [2]. Absorption and scattering of radio waves due to raindrops result in signal attenuation and in reduction of overall system availability and performance. These problems have forced the research community to balance the trade-off between bandwidth availabilities and rain attenuation issues at higher frequencies. The attenuation on any given path depends on the value of specific attenuation, frequency, polarization, temperature, path length, and latitude. The short integration time rainfall rate is the essential input parameter in the prediction models for rain attenuation. The local prediction model is analyzed in South Korea, where the modified polynomial model shows the predictable accuracy for estimation of 1-minute rainfall rate distribution [3–5]. Rain attenuation prediction models take into account the path reduction factor, which features both path length and rainfall rate. The product of the path

reduction factor and the physical path length of a microwave link is the effective path length which is defined as the intersection between the rain cell and the propagation path. It is observed that the effective path length is smaller than the actual physical path length, which leads to the introduction of the path reduction factor [6]. For the purpose of this paper, four established attenuation models have been utilized for the prediction of rain attenuation in South Korea. These are the ITU-R P.530-16 method [7], da Silva Mello model [8, 9], Moupfouma model [10], and Abdulrahman model [11]. The comparative study of terrestrial rain attenuation in the South Western geographical region of Nigeria has been performed through the application of those models. Abdulrahman proposed a prediction model which exhibited the overall best performance, and the da Silva Mello model seems to be the second preferable model [12]. Furthermore, performances of these models are analyzed in [13–15] which studied the suitable model for the prediction of rain attenuation in terrestrial links. Moupfouma [10] and Abdulrahman's [11] models are affected by use of the rainfall rate at 0.01% of the time with a 1-minute integration time, averaged over a period of three years. The comparative analyses of 1-minute rain rate measurement are further performed in [16]. Similarly, the studies of specific rain attenuation are analyzed for Ku and Ka band in [17–19]. Additionally, the differential equation approach is analyzed in [20] and the cumulative distributions of rain attenuation obtained from Praha, similar to climatic regions as of South Korea, are compared with the calculated ones in accordance with relevant ITU-R recommendation [21]. Moreover, the summary of the applicable path length in a terrestrial microwave link at temperate and tropical regions is studied in [22]. The remainder of the paper is organized as follows: "Background" summarizes the various techniques adopted for the study of rain attenuation prediction models in a terrestrial microwave link. "Methodology and Analyses of Experimental Data" illustrates the setup of the experimental system. The proposed approach is demonstrated in "Result and Discussion". Finally, "Conclusion" draws the conclusion of highly reliable statistical results.

2. Background

The rain-induced attenuation in a terrestrial path is expressed as the product of specific attenuation (dB/km) and the effective propagation path length (km). The rain attenuation A (dB) exceeded at p percent of time is calculated as

$$A = \gamma_R d_{\text{eff}} = \gamma_R dr. \tag{1}$$

Similarly, the specific attenuation, γ_R (dB/km) is obtained from the rain rate R (mm/h) using the power law relationship as

$$\gamma_R = kR^{\alpha}, \tag{2}$$

where k and α depend on the frequency and polarization of the electromagnetic wave. The constants appear in recommendation tables of ITU-R P.838-3 [23]. The values of k and α parameters for the present location at frequency 18 GHz under horizontal and vertical polarizations are 0.070784, 1.081827 and 0.077076, 1.002505, respectively. Similarly, r is the path reduction factor at the p time percentage and d is the radio path length in km.

2.1. ITU-R P.530-16 Model. This recommendation provides prediction methods for the propagation effects that should be taken into account in the design of digital fixed LOS links operating beyond 5 GHz, both in clear weather and in rainfall conditions. Additionally, it provides link design guidance in clear step-by-step procedures including the use of mitigation techniques to minimize propagation impairments. The final outage predicted is the base for other recommendations addressing error performance and availability. The method is based on the calculation of the behavior of path attenuation that exceeded for 0.01% of the time, which is the product of specific attenuation, γ_R (dB/km), and effective path length, d_{eff}, which depends on the product of actual path length, d, and path reduction factor, r. The attenuation that exceeded for other percentages of time in the range 0.001% to 1% is deduced from the power law whose expression and estimation of the factor, r, is given in the recommendation of ITU-R P.530-16 [7].

2.2. da Silva Mello Model. According to the da Silva Mello model, equivalent rain cells can intercept the link at any position with equal probability. This method uses the full rainfall rate distribution as input for predicting the rain attenuation cumulative distribution and is given by [9].

2.3. Moupfouma Model. According to Moupfouma, a terrestrial microwave link is described by its actual relay path length "L" which corresponds to the space between two ground stations. As the first step, this model takes the rainfall rate value at exceedance probability of 0.01% for the determination of induced rain attenuation that exceeded for the same percentage of time [10].

2.4. Abdulrahman Model. The method studied the relationship between path reduction factor and different link lengths by using multiple nonlinear regression techniques. In the analysis of the experimental data, the concept of equivalent rain cells has been retained where the relationship between equivalent rain cell diameter, d_0, and the corresponding rain rate at 0.01% of the time, $R_{0.01}$ [11], are taken into consideration.

3. Methodology and Analyses of Experimental Data

The microwave link at 18 GHz is installed between the transmitter station in Khumdang (37°8′8.41″N 127°30′56.16″E, Korea Telecom, KT station) tower and the receiver station in Icheon (37°8′49.57″N 127°32′54.82″E, National Radio Research Agency, RRA station) tower, at a separation distance of 3.2 km. Icheon is a city in Gyeonggi Province, South Korea, with the precipitation amount of above 300 mm for

TABLE 1: The 18 GHz link descriptions [24].

Descriptions	Specification
Antenna type	Front-fed parabolic
Frequency band (GHz)	17.7~18.2
Polarization (@ Khumdang, KT Station) tower	Vertical
Polarization (@ Icheon, RRA Station) tower	Vertical for antenna 1, horizontal for antenna 2
Maximum transmit power (W or dBm)	0.16 or +22
Reception method	Super heterodyne
Modulation	QPSK
Maximum modulation degree	8-bit/Hz
Radio throughput	367 Mbps
Electronic power and amplifier	Monolithic microwave integrated circuit (MMIC) with 12 VDC power supply and −10 dBm input signal
BER received threshold (for horizontal polarization) (dBm)	−52.3
BER received threshold (for vertical polarization) (dBm)	−32.8
Half power beam width	1.9°
Antenna for both transmitting and receiving side	
Size (m)	0.6
Gain (dBi)	38.8

the months of July and August. The availability of the terrestrial link for 2013, 2014, and 2015 was 99.99%, 98.96%, and 99.95%, respectively. The downtime is resulted due to the calibration in the receiver system during clear sky days and power failure. Similarly, the uptime of the OTT Parsivel for the mentioned three-year instances was 97.5%, 98.89%, and 99.95%, respectively. The downtime was because of the calibration and cleaning of the instrument whose specifications are tabulated in Table 1 as obtained from the system designer. The dynamic range of the receiver varies from 40 dBi to 75 dBi. The one antenna at the Khumdang KT Station tower is vertically polarized, and out of two antennas at the Icheon RRA Station tower, one antenna is vertically polarized and another is cross-polarized which receives its cross-polarization component due to big rain drops on horizontal polarization. Antennas are protected by radome to prevent wetting antenna conditions. These results act as a preliminary basis for understanding the effect of rain attenuation in horizontal and vertical polarization, but there is less reliability of measured data because the receiving path contains cross-polarization measurement which might create an inaccuracy due to large variation against the angle. However, the obtained raw data shall be a fundamental step to understanding the effect of rain attenuation.

Additionally, rain rate data are measured via an OTT Parsivel, a laser-based optical disdrometer for simultaneous measurement of particle size and fall velocity of all liquid and solid precipitation, for every 10-second interval over a 3-year period. The specifications of the OTT Parsivel disdrometer installed at the study site are given in Table 2.

The OTT Parsivel disdrometer produces a horizontal strip of light where the emitter and receiver are integrated into a single protective housing. As a hydrometeor falls through the laser beam, there is the change in the measured signal output voltage which determines the particle size.

TABLE 2: Technical specifications of the OTT Parsivel disdrometer (OTT) [25].

Features	Technical data
Measuring range (diameter)	0.2-25 mm
Beam size	180×30 mm
Measuring area	54 cm^2
Range of measurement velocity	0.2-20 m/s
Rain rate precipitation intensity	0.001-1200 mm/hr
Accuracy	±5% (liquid), ±20% (solid)
Power supply	10-36 V DC, reverse battery protection
Interfaces	RS 422/RS 485/SDI-12
Temperature range	−40 to +70°C

Similarly, particle speed is determined by the duration of the signal. After the determination of particle size and speed, OTT parsivel disdrometer bin measured particles into particle counts per velocity and diameter class in which it shall have 32 classes of drop size and velocities. The sensor on OTT Parsivel transmits all data to a PC through the RS-485 interface. An automatic heating system prevents ice buildup on the sensor heads which is maintained by a temperature sensor that measures the temperature for each second whose detail procedure is mentioned in [25–27]. The schematic diagram for the system setup is shown in Figure 1. As noticed in Figure 1, the front-fed parabolic antenna is mounted at 30 m height on the 35 m Khumdang KT Station tower. The outdoor unit is connected to the indoor unit via a coaxial cable which is of length of approximately 30 m. Similarly, two front-fed parabolic antennas are mounted at 15 m and 14 m on the Icheon RRA Station tower of 20 m where this tower is built on the 15 m building top, which is connected
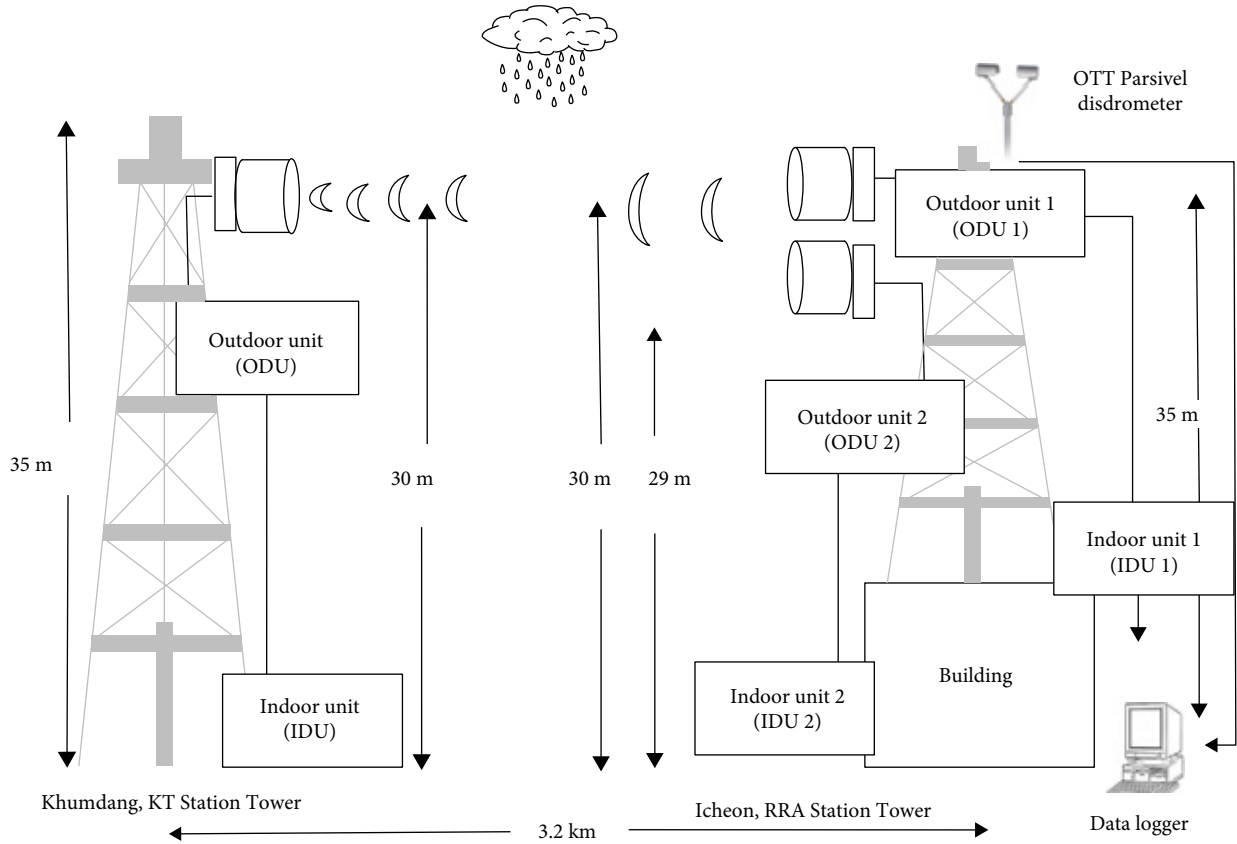
FIGURE 1: Experimental setup for rain attenuation and rain rate measurement [24].

to two separate outdoor units which are in turn connected to two indoor units via a 40 m coaxial cable. The height information shown in Figure 1 is the approximate values. Due to this system setup, there might be higher values of attenuation level as noted for horizontal and vertical polarizations. The data logger unit along with the OTT Parsivel rain gauge is set up in the Icheon RRA Station where a rain gauge is installed at top of the tower.

The path attenuation is calculated by finding the difference between RSL during clear sky conditions and the RSL during rainy conditions for horizontal and vertical polarized signals at various rain rates as follows [2]:

$$\text{Attenuation}(\text{dB}) = \text{RSL}_{\text{clear sky}} - \text{RSL}_{\text{rainy}}. \tag{3}$$

The monolithic microwave integrated circuit (MMIC) with a 12 VDC power supply and -10 dBm input signal which is built internally to the equipment support for the attenuation measurement with a radio throughput of 367 Mbps. In order to counteract the effects such as scintillation, an appropriate antenna size is chosen with a suitable range of frequencies as 17.7 to 19.7 GHz along with the minimum received signal level threshold as mentioned in Table 1 which is maintained at the receiving side. In order to process raw data, a similar approach as used for determining 1-minute rain rates in [28] is adopted to obtain the rain attenuation value for a 1-minute interval. The measured rain rate for

the 10-second time period is averaged to 60 seconds so as to obtain the required rain rate for a 1-minute period. Similarly, the raw data of the experimental 10-second rain attenuation is converted to 60 seconds of time period by taking the average of these 10-second data sets to a 60-second time period. These data are combined in descending order, and the required 1-minute rain rate and attenuation values along with the diameter of rain cell size are determined from 1% to 0.001% of the time. For instance, at 0.01% of the time, 1-minute rain rate and attenuation as well as rain cell diameter values are taken for about 158 $((3*365*24*60*0.01)/100 = 157.68 \approx 158)$ instances for the 3-year measurement when combined together. These instances are obtained by multiplying the number of experimental year and number of days in a year as well as hour and minute in a day, with required time percentage.

The cumulative distribution of the 1-minute rain rate calculated from the measured rain rate for the 10-second intervals for three years (2013 till 2015) of the studied location is shown in Figure 2. This figure indicates that the maximum rainfall rate occurred in 2013, but it decreases for successive years which might be due to the variability of rainfall occurrence in different seasons under mentioned periods. For instance, at 0.01% of the time, the obtained rainfall rate is 67.34 mm/hr in 2013 whereas in 2014 and 2015, the values are 35.48 and 36.07 mm/hr, respectively. The paper considered the combined value of the rainfall rate which indicates that at 0.01% of the time, the 1-minute
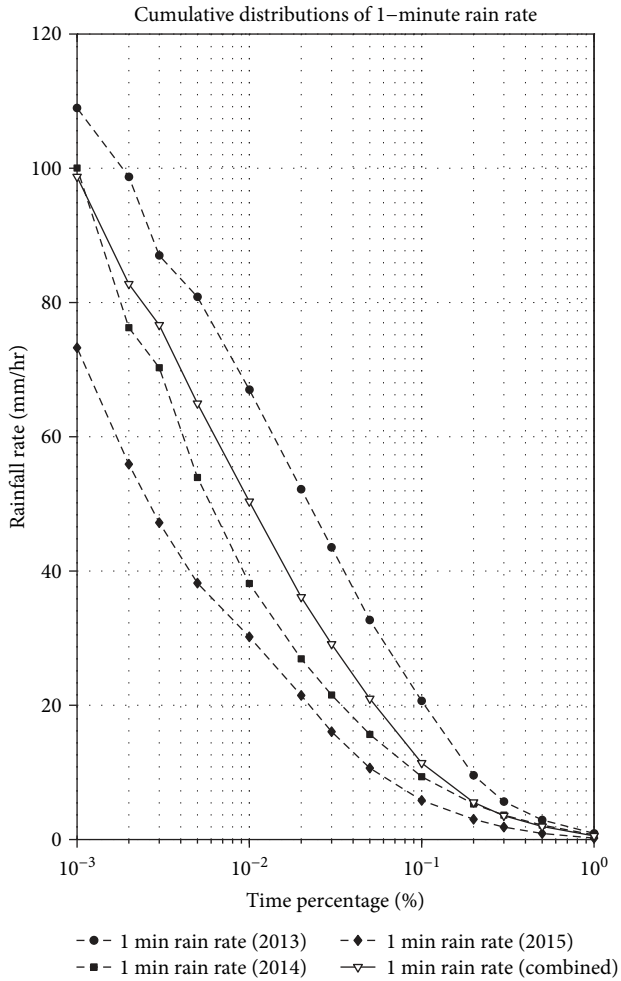
Cumulative distributions of 1–minute rain rate

FIGURE 2: Rainfall rate distribution at Icheon [24].

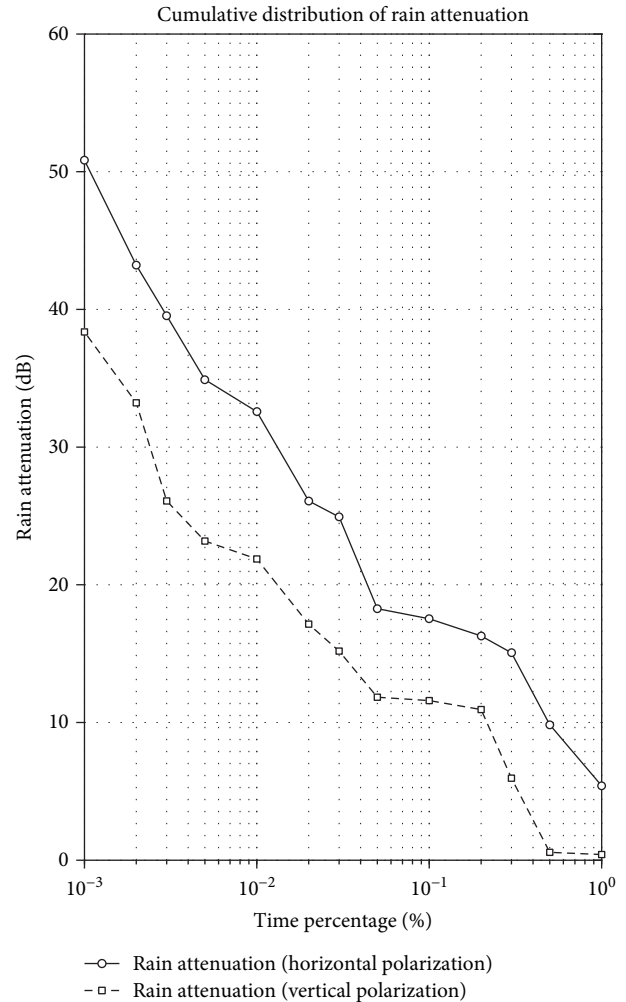Cumulative distribution of rain attenuation

FIGURE 3: Distribution of rain attenuation for various rain exceedance values at Icheon [24].

rainfall rate value is 49.79 mm/hr for the Icheon site. Furthermore, 1-minute rain rate values decrease and tend to be smaller for higher time percentages; for example, at 0.5% and 1% of the time, the rain rates are observed to be 1.99 mm/hr and 0.65 mm/hr, respectively. Similarly, at a lower time percentage the 1-minute rain rate is increased, for example, at 0.001% of the time the rain rate obtained is 98.57 mm/hr. As depicted in Figure 3, rainfall results in greater attenuation for horizontal polarization as compared to vertical polarization. This might be due to the cross-polarization measurement which can decrease the reliability of the measured values as the transmitter antenna gain at 90° fluctuates with small changes in angle. In addition, ITU-R P.530-16 also indicates a similar behavior as shown in Figure 4. The fundamental reason might be the effect of raindrops, which are usually oblate which offers greater extinction to horizontal polarization compared to the vertical one. Furthermore, some discretized nature in the generated curves might be due to the irregular arrangement of the measured 10-second interval data. In some instances, the data are sampled in 5 seconds whereas in most cases, it is sampled in 10 seconds. Thus, we have presented the measurement data which are combined for 1-minute

distribution. The data sets are arranged for 1% to 0.001% of the time as per the recommendation of ITU-R P.311-15 [29]. During horizontal and vertical polarization, at 0.01% of the time, the obtained rain attenuation values are 32.57 and 21.88 dB, respectively. Interestingly, while using k and α which are obtained from ITU-R P.838-3, the expected maximum attenuation is found to be 15.4 and 12.3 dB for horizontal and vertical polarization, respectively, which depicts that the measurement results are higher than predicted values. This might be because of not considering the effect of the effective path length, d_{eff}, for the derivation of total attenuation as well as the arrangement of measured data from 10-second and 5-second intervals which are combined to a 1-minute instance. Similarly, the rain attenuation values increased for a lower time percentage which reached up to 50.83 and 38.36 dB at 0.001% of the time whereas at a higher time percentage as such for 1% of the time, the rain attenuation value decreased to 5.40 and 0.41 dB for horizontal and vertical polarization, respectively.

The rain cell diameter is typically 100 m to 15 km, but we have analyzed the equivalent or effective rain cell diameter as mention in equation (4). The rain cell size is calculated for
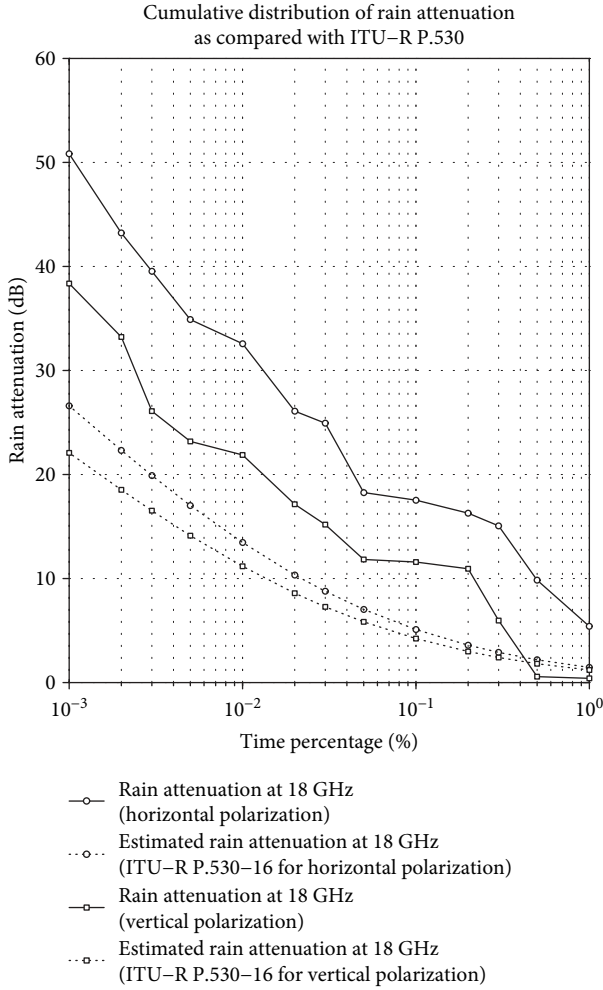
Figure 4: Cumulative distribution of rain attenuation compared with ITU-R P.530-16 for various integration times [34].

the 60-second period from the experimental measurement of 10-second instance. Due to this arrangement, the measurement result shows a higher value as 190 mm. This shows the increment of rain cell size for the 60-second period as shown in Figure 5 whose values for the defined time instances are depicted in Table 3.

However, the work performed in Climpara [30] and Radio Africa [31] points to the fact that peak rain rates in a cell increase, and the cell size reduces while for lower peak rain rates, the cell diameter increases. Similarly, the extensive work undertaken by Dr. Apolonia Pawlina Bonati et al. [32] shows that the dynamics and rain cell structures are generally statistically invariant. This is further explained in [33] by Tharek et al. for the determination of the path reduction factor that pertains to the input data into the four models as mentioned in Section 2. This profile is better estimated by a power law equation which is expressed as

$$d_0 = 106.8 \, R_p^{-0.1125}, \tag{4}$$

where R_p and d_0 are the 1-minute rainfall rate and equivalent diameter of rain cell size, respectively. The effective rain cell
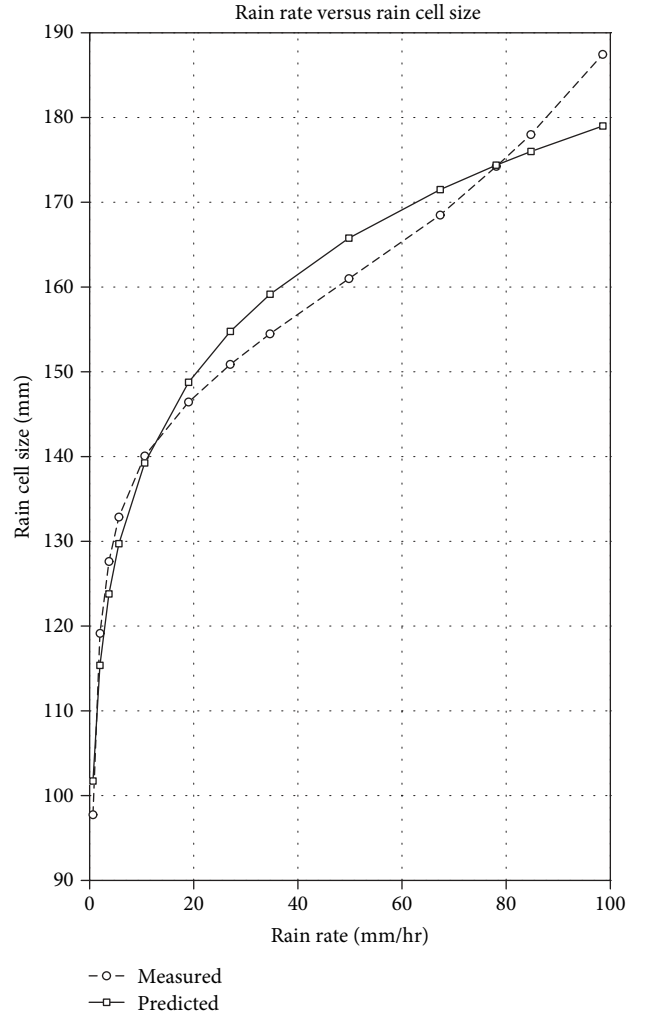

Figure 5: Distribution of rain cell size against rain rate [24].

Table 3: Observed rain rate and calculated rain cell size.

Time instance (%)	Observed rain rate (mm/hr)	Calculated rain cell size (millimetre)
0.1	10.58	139.25
0.01	49.79	165.77
0.001	98.57	179.01

size has been analyzed against the rain rate over the tropical climate [33]. The regression value of R^2 is 0.9738 which is close to unity which signifies its better accuracy in estimation of the diameter of rain cell size. However, the $R_p^{-0.1125}$ factor in the fitted expression is an inverse $1/x$ relationship which might not explain the shape of the curve with $x^{0.5}$ family of curves. But these empirically derived coefficient values as obtained from the curve-fitting procedure performed from the Matlab program [34] shows the preliminary step to characterizing the relationship between rain cell size and 1 min rain rate distribution. Figure 6 shows the plot of rain attenuation against the rain rate for the experimental links
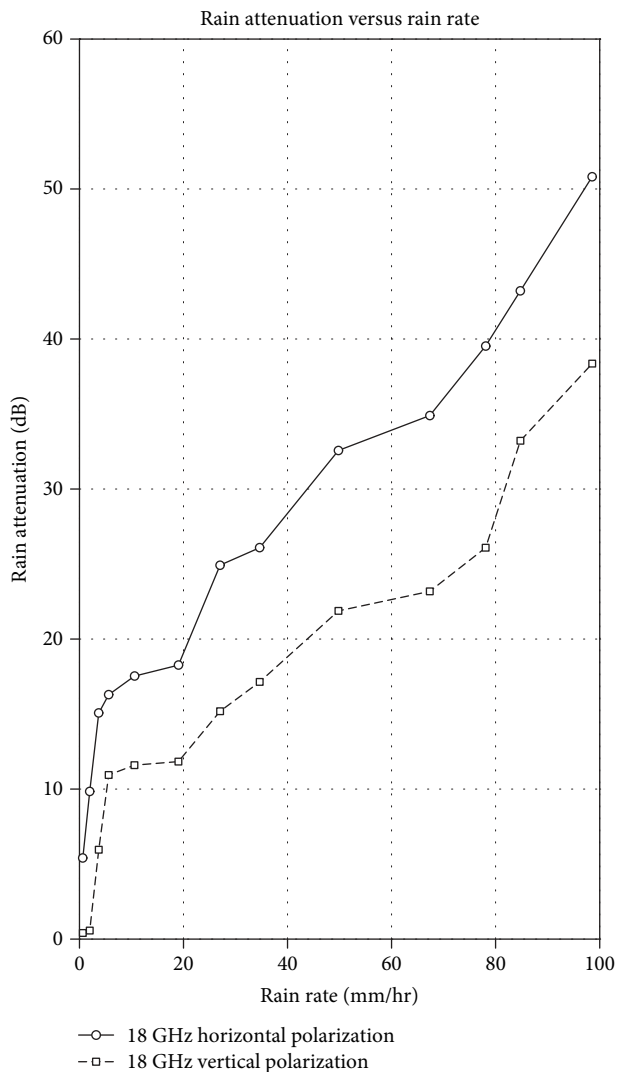
Figure 6: Rain attenuation against rain rate [24].

of 18 GHz. This figure highlights the fact that rain attenuation is more prominent in horizontal polarization as compared to vertical polarization. For instance, in the 49.79 mm/hr rain rate, the measured rain attenuation values are 32.57 and 21.88 dB for 18 GHz horizontal and vertical polarization, respectively.

A similar experimental setup is established for the same link distance of 3.2 km in 38 GHz whereas the shorter link distance of 0.1 km is considered for the 75 GHz link between the Icheon tower (37°8′49.57″N 127°32′54.82″E) and the EMS Dong Yoksang station (37°11′49.2″N 127°25′33.6″E) [35]. Figure 7 shows the schematic diagram of the system setup. As noticed from Figure 7, one front-fed parabolic antenna is mounted on the 35 m high Khumdang KT Station tower in the 38 GHz operation link. The coaxial cable of 29 m is used for maintaining the connection between the outdoor unit (ODU) and the indoor unit (IDU). On the other hand, two parabolic antennas are mounted on the 20 m high Icheon RRA Station tower under vertical polarization, for the 38 and 75 GHz links. This is set up on the 15 m high building

rooftop. Similarly, the separate 46 m coaxial cable is used to connect the ODU of 38 and 75 GHz operating antenna to IDU. The front-fed parabolic antenna is maintained in the EMS Dong Yoksang Station tower which is connected to the IDU through the ODU via a 5 m coaxial cable. This station lies on a hilly part with the tower lying on the rooftop of the building of around 10 m height. The shorter cable is required because this station lies on the rooftop of the building. The height information is the approximate values. The data logger unit along with the OTT Parsivel rain gauge is set up at the Icheon RRA Station which maintains the database of the measured rain attenuation and rain rate.

Furthermore, the measured 1-minute rain rate as obtained from RRA is compared with the rain rate derived from the 1-minute rainfall amount experiment conducted by Korea Meteorological Administration (KMA) in the Icheon (37.27°N, 127.45°E) region, where the rain rates differ by about 10 mm/hr for 0.01% of the time which might be due to the different experimental procedures. The detailed operation of the KMA experiment is mentioned in [3, 4]. Unfortunately, the KMA experiment is conducted to measure only the 1-minute rainfall amount where the measurement of rain attenuation is not conducted. However, this 1 min rainfall amount experiment is significant for the comparison of the 1-minute rain rate conducted by RRA. The experimental 1-minute rainfall amounts are combined for respective 5-minute, 10-minute, 20-minute, 30-minute, and 60-minute instances. These raw data are arranged in descending order, and the respective rainfall amount is noted for a given time percentage. Thus, the achieved rainfall amount at diverse time instances are converted to rain rate following the approach presented in [36]. For instance, at 0.01% of the time, 1-minute, 5-minute, 10-minute, 20-minute, 30-minute, and 60-minute rain rates are taken for about 526 $((10^*365^*24^*60^*0.01)/100 = 525.6 \approx 526)$, 105 $((10^*365^*24^*12^*0.01)/100 = 105.12 \approx 105)$, 53 $((10^*365^*24^*6^*0.01)/100 = 52.56 \approx 53)$, 26 $((10^*365^*24^*3^*0.01)/100 = 26.28 \approx 26)$, 18 $((10^*365^*24^*2^*0.01)/100 = 17.52 \approx 18)$, and 9 $((10^*365^*24^*1^*0.01)/100 = 8.76 \approx 9)$ instances for the 10-year measurement performed by KMA. These instances are obtained by multiplying the number of experimental year and number of days in a year as well as hour and minute in a day, with required time percentage. These values are taken as an input parameter along with the latitude and longitude information so as to obtain the 1-minute rain rate from software recommended by ITU-R P.837-6 [37]. This indicates that for higher time conversions, particularly at 20, 30, 60 minutes to 1 minute, ITU-R P.837-6 shows the overestimation whereas for lower time conversions from 5 and 10 minutes to 1 minute, this model gives a closer prediction against the calculated 1-minute rain rate values. This signifies that the measured values of the rainfall rate as provided by RRA are underestimated, which is used as an input data for the prominent prediction models. This might be the reason that most of the prediction models generate lower values against the measured attenuation in the 18 GHz terrestrial link for horizontal and vertical polarization. Hence, the rain rate measurement of longer duration is required for efficient analyses. The use of the ITU-R P.837-6 approach
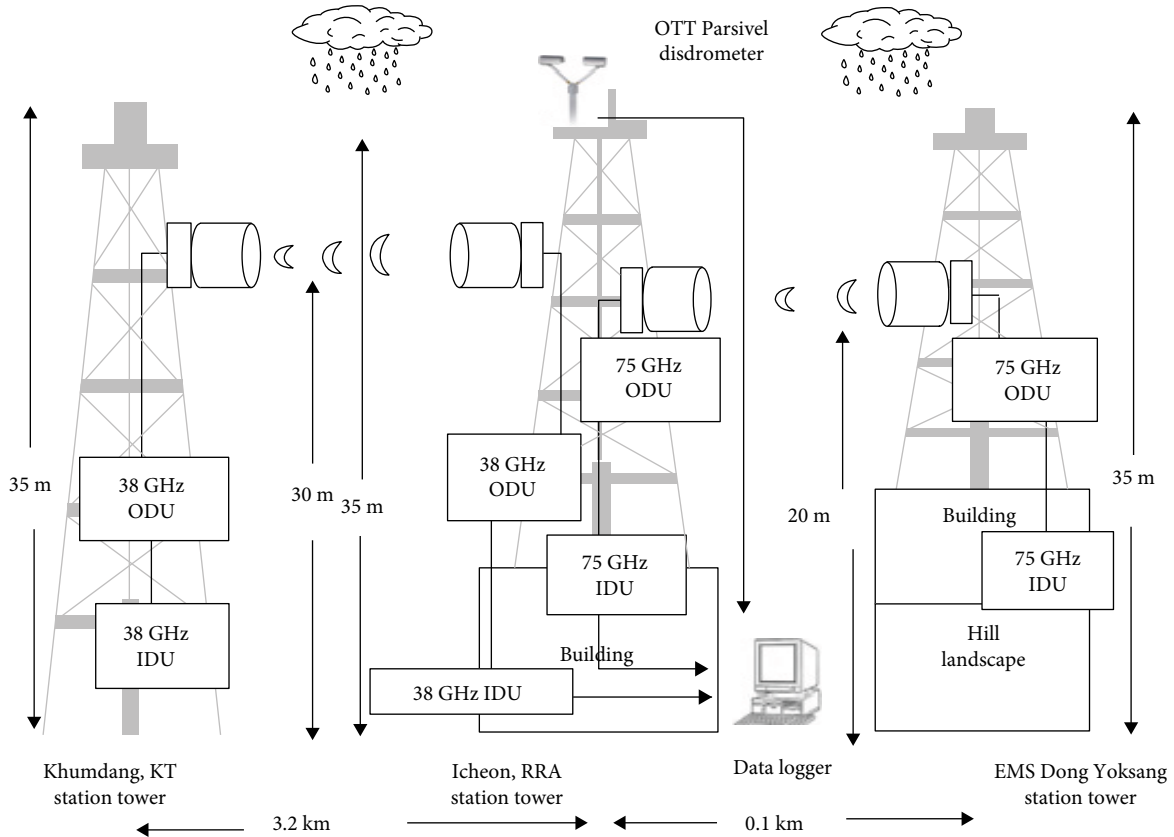
FIGURE 7: Experimental setup for rain attenuation and rain rate measurement [24].

for the estimation of the rain rate is calculated from the measured 1-minute rainfall amount which was performed through a tipping bucket rain gauge instrument due to which the estimated rain rate is significantly higher and it could not be used for better attenuation values. In order to have a better 1-minute rain attenuation estimation, the input 1-minute rain rate should be performed in mm/hr. This has been performed by RRA for a 1-minute rain rate through the OTT Parsivel disdrometer.

4. Result and Discussion

The comparison between measured rain attenuation complementary cumulative distribution function (CCDF) against ITU-R P.530-16 predicted values for several time percentages at an equiprobable exceedance probability ($0.001\% \leq P \leq 1\%$) are plotted in Figure 4. This shows that the ITU-R P.530-16 method does not accurately estimate the rain attenuation CCDF even though this model gives fair statistics at a higher time percentage ($P \geq 0.5\%$). At a higher time percentage, this model dramatically underestimates the measured rain attenuation. For instance, at 0.01% of the time, the measured rain attenuation values are 32.57 and 21.88 dB for the 18 GHz horizontal and vertical links, respectively. While the corresponding ITU-R P.530-16 estimated values are 13.47, 11.18 dB, respectively. The reason behind this difference could be the fact that the matrices used to obtain the parameters might have low spatial resolution and the rain

rate used at 0.01% of the time as an input parameter might be of lower values. In addition, ITU-R P.530-16 considers additional propagation effects, e.g., atmospheric gases, sand storm, and diffraction effects which are neither computed nor measured as part of the experiment setup and comparison which might have resulted in an underestimated nature. On this discrepancy, there is the immediate need for a rain attenuation prediction model that can provide a relationship against the local 1-minute rain distribution. Under this aspect, the paper presents a new approach that shall be applicable in analyzing the 1-minute rain attenuation distribution pattern for terrestrial microwave links, particularly for a lower microwave frequency, by considering the effective rain rate and diameter of the rain cell size approach.

As an initial step, the relationship between theoretical specific rain attenuation as specified by ITU-R P.838-3 [23], $\gamma_{\%p}$, and effective specific rain attenuation, γ_{eff}, is obtained by dividing the experimentally derived rain attenuation values by the product of the link distance and path correction factor. The methods as adopted in [9] have been used but with some variation on the effective rain rate. The plot between these two parameters is shown in Figure 8 which shows the increasing curve nature for both horizontal and vertical polarizations. The empirical relationship between these two quantities is given by the following ratio:

$$\frac{\gamma_{\text{eff}}}{\gamma_{\%p}} = \frac{kR_{\text{eff}}^a}{kR_{\%p}^a}. \tag{5}$$
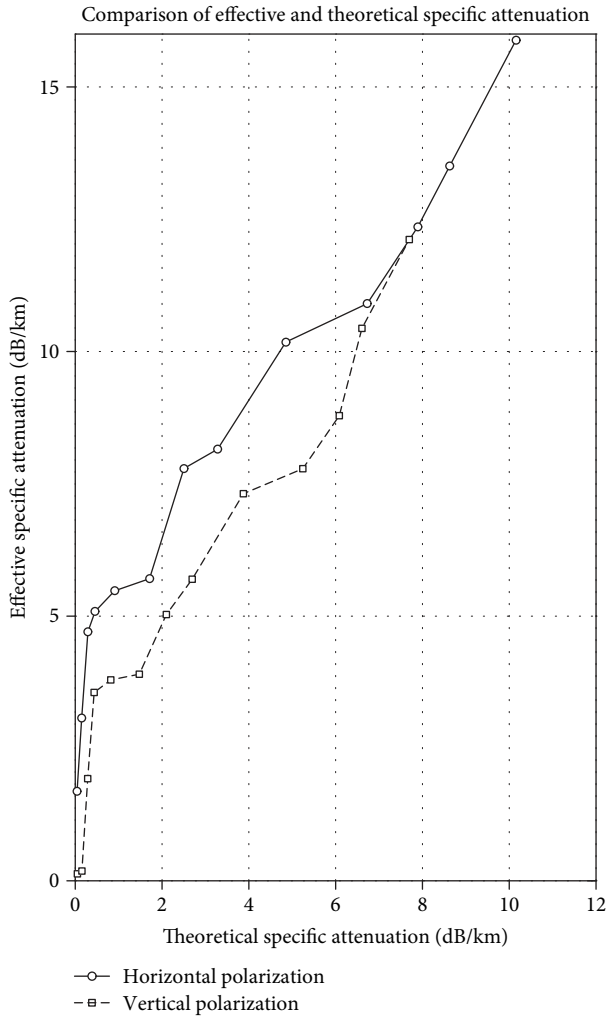
FIGURE 8: Comparison of effective and theoretical specific rain attenuation [34].

Solving equation (5), we get the effective rain rate as

$$R_{\text{eff}} = \left(\frac{1}{k}\gamma_{\text{eff}}\right)^{1/\alpha} = R_{\%p}\left(\frac{\gamma_{\text{eff}}}{\gamma_{\%p}}\right)^{1/\alpha}. \quad (6a)$$

Alternatively, the effective rain rate can be expressed as a function of measured rain rate by power law as follows:

$$R_{\text{eff}} = aR_{\%p}^{b}, \quad (6b)$$

where a and b are derived empirically whose values are 18.24, 0.4318 and 8.719, 0.6162, respectively, for horizontal and vertical polarization. The inhomogeneity of specific rain attenuation over the path length has been accounted by the inhomogeneity in rain rate. In order to generalize the proposed approached method, the experimental links performed at 38 and 75 GHz are considered. A similar method is adopted to calculate the effective rain rate for these higher microwave links. The empirically derived values of a and b for the 38 and 75 GHz links are 1.458, 0.7846 and 179.9,

0.655, respectively. Under the presence of effective specific rain attenuation, equation (6a) has been used for the derivation of the effective rain rate. Hence, the effective rain rate is derived from the effective specific rain attenuation. The effective specific rain attenuation can be calculated by dividing the experimentally derived rain attenuation values with the product of actual link distance and path correction factor as mentioned earlier. It is observed that the effective path length is smaller than the actual physical path length, which leads to the introduction of the path correction factor as mentioned in [6]. The path correction factor, r, is given by

$$r = \frac{1}{1 + (d/d_0(Rp))}, \quad (6c)$$

where d is the actual link distance and $d_0(R_p)$ is the equivalent rain cell diameter given by equation (4) which depend on the 1-minute rain rate exceeded at $\%p$ of the time.

In addition, the proposed approach as represented by equation (6b) can be used to derive the effective rain rate from 1-minute rain rate values for the $\%p$ time percentage. This approach is adopted for further analysis because it utilizes the full 1-minute rain rate distribution over $0.001\% \leq \%p \leq 1\%$. The rain rate considered for further part is the 1-minute rain rate distribution. Therefore, the attenuation exceeded at $\%p$ of the time can be expressed as given in equation (6d),

$$A_{\%p} = \gamma_{\text{eff}}d_{\text{eff}} = k\left[R_{\text{eff}}\left(R_{\%p}, d\right)\right]^{\alpha}\left[\frac{d}{1 + (d/d_0(R_{\%p}))}\right]. \quad (6d)$$

This shows that the modeling approach is simpler which incorporates the inhomogeneity of rainfall by considering the effective rain rate which is limited to a certain climatic area. The effective specific attenuation or effective rain rate is introduced with the consideration of local measurement analysis. The experimental setup is performed for the particular location whose data for the 1-minute rain rate and rain attenuation are studied to propose the attenuation exceeded for $\%p$ of the time. A more informative experiment should be involved with several longer paths along with other lower frequency ranges as well as the study of rain attenuation in diverse locations of South Korea. The National Radio Research Agency (RRA) is planning for establishment of these systems in other locations in the near future for better prediction of rain attenuation models. Hence, this approach shows suitability only in the mentioned location. As a preparatory step, several prominent rain attenuation models as well as the proposed approach are analyzed. These are shown in Figures 9(a) and 9(b) for 18 GHz horizontal and vertical polarization, respectively. Due to the dependency on the experimental system, the derived coefficients for equation (6b) are tested in the mentioned location for the 18 GHz link only and promising results are obtained to support the study of prominent 1-minute rain attenuation models for lower frequency. The following section clarifies the scientific argument to support the findings.
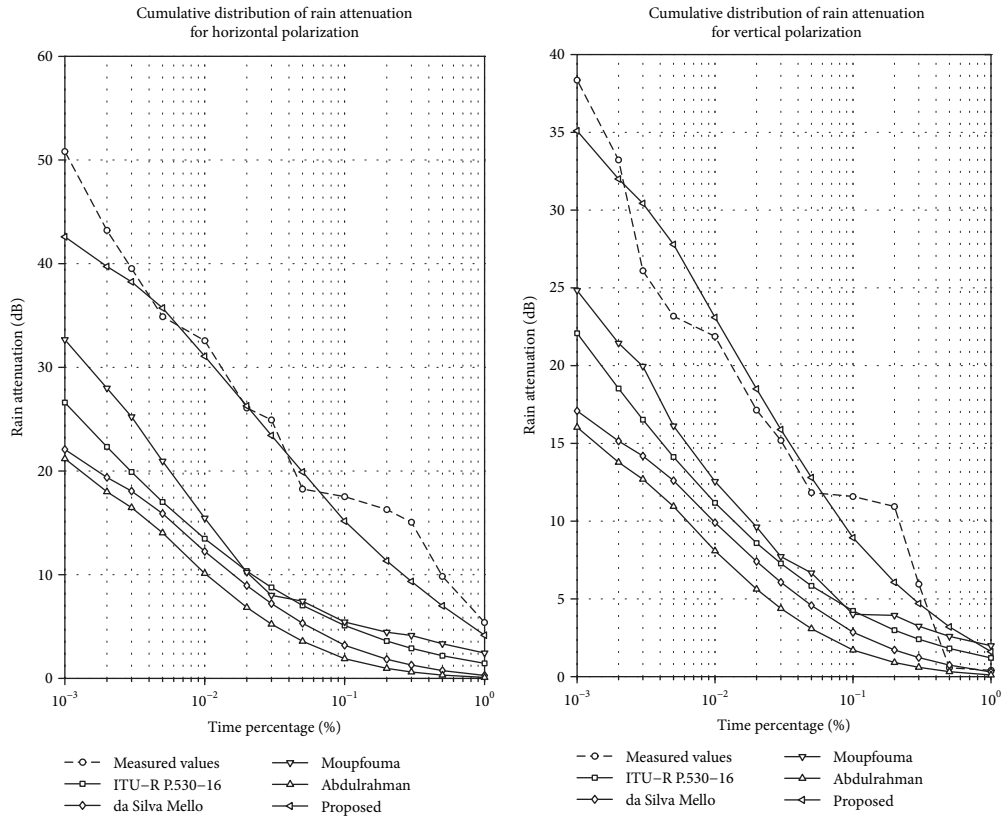
(a)

(b)
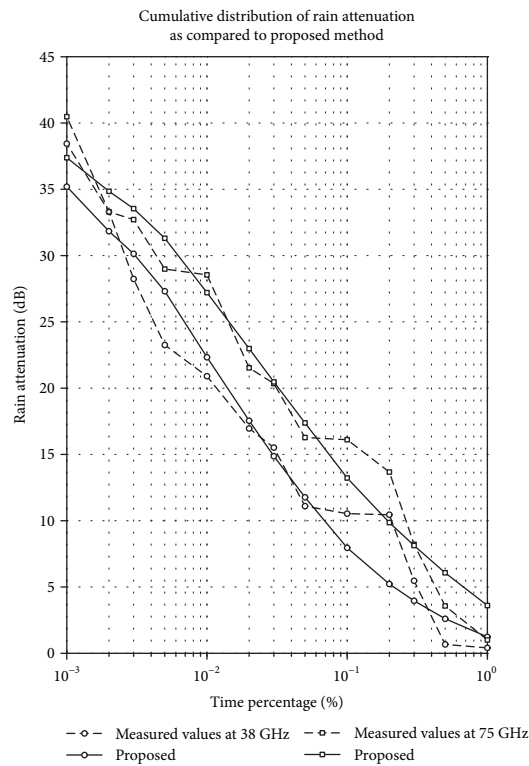
(c)

Figure 9: (a) Comparison of measured and predicted attenuation for horizontal polarization. (b) Comparison of measured and predicted attenuation for vertical polarization. (c) Comparison of measured and predicted attenuation for 38 and 75 GHz [34].

Figures 9(a) and 9(b) show the plots of the proposed approach and of the ITU-R P.530-16, da Silva Mello, Moupfouma, and Abdulrahman models for horizontal and vertical polarization, respectively. The attenuation value is higher at the present location as compared to the prediction of other models which might be due to a nonuniform distribution of the rainfall rate that results in the links to experience different depths of attenuation. Additionally, the measurements are performed for the 10-second instance of time period due to which there might be a degradation in the signal-to-interference ratio owing to events in which the desired signal is subjected to higher attenuation than the interfering signals. Furthermore, the models predict rain attenuation based on only the rainfall rate for 0.01% of an average year which has resulted in the underestimation of the rain attenuation statistics against the measured results. Even though the role of the interfering signal in causing attenuation of the desired signal is not pertinent here, the higher attenuation could be due to the higher effective rain rates for different time percentages as compared to that predicted by the other models.

The underestimation becomes highly pronounced at a lower time percentage. For instance, the measured attenuation values are 17.53, 32.57, and 50.83 dB and 11.59, 21.88, and 38.36 dB, respectively, for horizontal and vertical polarization at 0.1%, 0.01%, and 0.001% of the time while ITU-R P.530-16 predicts 5.10, 13.47, and 26.61 dB and 4.23, 11.18, and 22.08 dB. A similar pattern is observed with the application of the da Silva Mello and Abdulrahman models which underestimate the measured cumulative statistics of rain attenuation. For instance, under horizontal and vertical polarization, da Silva Mello predicts 3.19, 12.24, and 22.08 dB and 2.85, 9.89, and 17.09 dB, respectively, at 0.1%, 0.01%, and 0.001% of the time whereas Abdulrahman predicts 1.89, 10.12, and 21.19 dB and 1.71, 8.09, and 16.03 dB, respectively. More underestimation is observed from the application of the Abdulrahman model. Although the Moupfouma model underestimates the measured cumulative statistics of rain attenuation, this model predicts relatively higher rain attenuation values as compared to the ITU-R P.530-16, da Silva Mello, and Abdulrahman models. For instance, the Moufouma model predicts 4.01, 13.22, and 24.14 dB and 4.01, 12.55, and 24.83 dB, respectively, for horizontal and vertical polarization at 0.1%, 0.01%, and 0.001% of the time. The difference of about 0.67 dB is noted for 0.01% of the time whereas for horizontal and vertical polarization, it is observed to be of about 19 and 9 dB, respectively, against the measured attenuation values. The proposed approach gives a very close estimation to measured cumulative statistics of rain attenuation. For instance, the proposed approach predicts 15.18, 31.07, and 42.59 dB and 8.93, 23.09, and 35.19 dB at 0.1%, 0.01%, and 0.001% of the time, respectively, for horizontal and vertical polarization. Unfortunately, the performance of the proposed approach is limited for a site-specific location and its validity required more tests and analyses of the experimental database performed for other locations. The better performance analysis of suitable methods is done from the error analysis in the further part. In order to measure the effectiveness of the

proposed approach, the method as depicted by equation (6d) has been used for 38 and 75 GHz links, with vertical polarization whose plots are shown in Figure 9(c).

As shown in Figure 9(c), the proposed approach generates better estimation to the measured cumulative statistics of rain attenuation for 38 and 75 GHz. For instance, the proposed approach predicts 7.96, 22.34, and 35.19 dB and 13.22, 27.21, and 37.38 dB at 0.1%, 0.01%, and 0.001% of the time, respectively, for 38 and 75 GHz against the measured values of 10.53, 20.89, and 38.44 dB and 16.11, 28.55, and 40.48 dB. Hence, the proposed approach shows some feasibility in other links and path lengths. The further error analysis shows the effectiveness of the proposed approach.

Goodness of fit is done through the calculation of relative error variables ($\varepsilon(P)$), standard deviation (STD), and root mean square (RMS) values whose values are tabulated at fixed probability levels when $0.001\% \leq \%p \leq 1\%$ as recommended in ITU-R P.311-15 [29]. The relative error probability used to access the models performance is given by

$$\varepsilon(P)_T = \frac{A_{\%p,\text{predicted}} - A_{\%p,\text{ measured}}}{A_{\%p,\text{ measured}}} \times 100 \quad [\%], \qquad (7)$$

where $A_{\%p,\text{predicted}}$ and $A_{\%p,\text{measured}}$ are the predicted and measured rain attenuation values, respectively, at the same probability level P, in the percentage interval $10^{-3}\% < P < 1\%$. Similarly, for STD and RMS calculation, the approaches followed in [3] have been adopted. The results for each method are listed in Tables 4(a) and 4(b) for 18 GHz under horizontal and vertical polarization, respectively.

Similar statistical results are obtained for 18 GHz under the horizontal and vertical polarization conditions. As noted from Tables 4(a) and 4(b), the ITU-R P.530-16, Moupfouma, and proposed approaches show a higher relative error when $0.5\% \leq P \leq 1\%$ which is justified from increased STD and RMS values whereas for lower time percentage when $0.001\% \leq P \leq 0.3\%$, there are lower values of relative error probabilities which is supported by the decreasing STD and RMS values. On the other hand, the da Silva Mello and Abdulrahman models give a lower relative error when $0.5\% \leq P \leq 1\%$ which is justified from decreased STD and RMS values. Thus, for a higher time percentage when $0.5\% \leq P \leq 1\%$, the da Silva Mello and Abdulrahman models can be used for estimation of rain attenuation under horizontal and vertical polarization. In addition, for a lower time percentage when $0.001\% \leq P \leq 0.3\%$, the ITU-R P.530-16, da Silva Mello, Moupfouma, and Abdulrahman models give higher relative error values which underestimate the measured cumulative rain attenuation statistics. Particularly, a lower underestimation is observed in case of the ITU-R P.530-16 and Moupfouma models. For instance, for horizontal and vertical polarization, ITU-R P.530-16 shows relative error percentages of 71%, 59%, 48% and 64%, 49%, 42% while these are 82%, 62%, 57%; 69%, 53%, 36%; 89%, 69%, 58% and 75%, 55%, 55%; 65%, 43%, 35%; and 85%, 63%, 58% for the da Silva Mello, Moupfouma, and Abdulrahman models at 0.1%, 0.01%, and 0.001% of the time, respectively. Additionally, the proposed approach shows relatively lower

TABLE 4

(a) Percentage error obtained after testing over the interval [0.001% to 1%] for horizontal polarization

Methods (horizontal polarization)	Parameters	Time percentage (%p)													ITU-R P.311-15		
		1	0.5	0.3	0.2	0.1	0.05	0.03	0.02	0.01	0.005	0.003	0.002	0.001	μv	σv	ρv
ITU-R P.530-16	ε(P)	−0.73	−0.78	−0.81	−0.78	−0.71	−0.61	−0.65	−0.60	−0.59	−0.51	−0.50	−0.48	−0.48	−1.04	0.33	1.1
	STD	0.10	0.15	0.17	0.15	0.08	0.02	0.02	0.03	0.05	0.12	0.14	0.15	0.16			
	RMS	3.95	7.66	12.16	12.69	12.43	11.23	16.16	15.74	19.10	17.88	19.63	20.89	24.22			
da Silva Mello	ε(P)	−0.95	−0.92	−0.91	−0.89	−0.82	−0.71	−0.71	−0.66	−0.62	−0.54	−0.54	−0.55	−0.57	−1.48	0.7	1.64
	STD	0.23	0.20	0.19	0.16	0.10	0.01	0.01	0.07	0.10	0.18	0.18	0.17	0.16			
	RMS	5.12	9.10	13.78	14.44	14.34	12.95	17.72	17.15	20.33	19.00	19.00	23.83	28.75			
Moupfouma	ε(P)	−0.55	−0.66	−0.73	−0.73	−0.69	−0.59	−0.68	−0.61	−0.53	−0.40	−0.40	−0.35	−0.36	−0.85	0.31	0.91
	STD	0.01	0.10	0.17	0.17	0.13	0.04	0.12	0.05	0.03	0.16	0.16	0.20	0.20			
	RMS	2.96	6.50	10.92	11.84	12.09	10.82	16.92	15.86	17.12	13.95	13.95	15.22	18.16			
Abdulrahman	ε(P)	−0.98	−0.97	−0.96	−0.94	−0.89	−0.80	−0.79	−0.74	−0.69	−0.60	−0.60	−0.58	−0.58	−1.89	1	2.14
	STD	0.20	0.19	0.18	0.16	0.11	0.03	0.01	0.04	0.09	0.18	0.18	0.19	0.19			
	RMS	5.31	9.53	14.45	15.33	15.64	14.69	19.70	19.25	22.45	20.86	20.86	25.21	29.64			
Proposed	ε(P)	−0.23	−0.29	−0.38	−0.30	−0.13	0.09	−0.06	0.01	−0.05	0.02	0.02	−0.08	−0.16	−0.14	0.16	0.22
	STD	0.11	0.17	0.26	0.18	0.01	0.21	0.06	0.13	0.08	0.15	0.15	0.04	0.04			
	RMS	1.24	2.85	5.71	4.95	2.35	1.65	1.50	0.19	1.50	0.83	0.83	3.49	8.23			

(b) Percentage error obtained after testing over the interval (0.001% to 1%) for vertical polarization

Methods (vertical polarization)	Parameters	Time percentage (%p)													ITU-R P.311-15		
		1	0.5	0.3	0.2	0.1	0.05	0.03	0.02	0.01	0.005	0.003	0.002	0.001	μv	σv	ρv
ITU-R P.530-16	ε(P)	1.96	2.18	−0.60	−0.73	−0.64	−0.51	−0.52	−0.50	−0.49	−0.39	−0.37	−0.44	−0.42	−0.52	0.53	0.74
	STD	2.07	2.29	0.48	0.61	0.52	0.39	0.41	0.39	0.38	0.28	0.25	0.33	0.31			
	RMS	0.80	1.24	3.55	7.95	7.36	6.00	7.91	8.55	10.70	9.06	9.57	14.69	16.28			
da Silva Mello	ε(P)	−0.27	0.30	−0.79	−0.84	−0.75	−0.61	−0.60	−0.57	−0.55	−0.46	−0.46	−0.54	−0.55	−0.85	0.5	0.98
	STD	0.25	0.81	0.28	0.33	0.24	0.10	0.09	0.05	0.03	0.06	0.06	0.03	0.04			
	RMS	0.11	0.17	4.73	9.22	8.74	7.26	9.12	9.73	11.98	10.57	11.90	18.07	21.28			
Moupfouma	ε(P)	3.89	3.55	−0.46	−0.64	−0.65	−0.44	−0.49	−0.44	−0.43	−0.30	−0.24	−0.35	−0.35	−0.37	0.56	0.67
	STD	3.69	3.34	0.66	0.84	0.86	0.64	0.70	0.64	0.63	0.51	0.44	0.56	0.56			
	RMS	1.58	2.02	2.72	7.00	7.58	5.16	7.47	7.52	9.33	7.06	6.14	11.78	13.53			
Abdulrahman	ε(P)	−0.74	−0.44	−0.90	−0.92	−0.85	−0.74	−0.71	−0.67	−0.63	−0.53	−0.51	−0.59	−0.58	−1.19	0.6	1.33
	STD	0.07	0.24	0.22	0.24	0.17	0.06	0.03	0.01	0.05	0.15	0.16	0.09	0.10			
	RMS	0.30	0.25	5.36	10.03	9.88	8.75	10.80	11.52	13.79	12.23	13.40	19.44	22.33			

TABLE 4: Continued.

Methods (vertical polarization)	Parameters	Time percentage (%p)													ITU-R P.311-15		
		1	0.5	0.3	0.2	0.1	0.05	0.03	0.02	0.01	0.005	0.003	0.002	0.001	μv	σv	ρv
Proposed	$\varepsilon(P)$	2.95	4.62	-0.21	-0.45	-0.23	0.08	0.05	0.08	0.06	0.20	0.17	-0.04	-0.09	0.08	0.38	0.39
	STD	2.40	4.06	0.76	1.00	0.78	0.47	0.51	0.47	0.50	0.35	0.39	0.59	0.64			
	RMS	2.95	4.62	0.21	0.45	0.23	0.08	0.05	0.08	0.06	0.20	0.17	0.04	0.09			

(c) Percentage error obtained after testing over the interval (0.001% to 1%) for 38 and 75 GHz

Methods (vertical polarization)	Parameters	Time percentage (%p)													ITU-R P.311-15		
		1	0.5	0.3	0.2	0.1	0.05	0.03	0.02	0.01	0.005	0.003	0.002	0.001	μv	σv	ρv
Proposed under 38 GHz	$\varepsilon(P)$	2.03	2.91	-0.28	-0.50	-0.24	0.06	-0.04	0.03	0.07	0.17	0.07	-0.04	-0.08	0.03	0.36	0.36
	STD	1.71	2.59	0.60	0.82	0.56	0.26	0.36	0.29	0.25	0.15	0.25	0.36	0.40			
	RMS	0.83	1.94	1.51	5.22	2.58	0.66	0.64	0.59	1.44	4.06	1.90	1.47	3.25			
Proposed under 75 GHz	$\varepsilon(P)$	2.57	0.70	-0.01	-0.28	-0.18	0.07	0.01	0.07	-0.05	0.08	0.03	0.05	-0.08	0.07	0.27	0.28
	STD	2.35	0.47	0.24	0.51	0.41	0.16	0.22	0.16	0.28	0.15	0.20	0.18	0.31			
	RMS	2.60	2.50	0.09	3.81	2.89	1.10	0.13	1.45	1.34	2.32	0.83	1.55	3.09			

relative error percentage values which is justified from decreased STD and RMS values. For instance, the proposed approach shows relative error percentages of 13%, 5%, 16% and 23%, 6%, 9% at 0.1%, 0.01%, and 0.001% of the time for horizontal and vertical polarization, respectively. Thus, the proposed approach shows a suitable estimation of rain attenuation for a specific site. But this still lacks clear justification due to the limited data sources. Although the proposed approach is equally applicable for the estimation of rain attenuation statistics at a lower time percentage when $0.001\% \leq P \leq 0.3\%$ of the time, its applicability to other regions still needs to be verified. Under this scenario, the ITU-R P.530-16 and Moupfouma models seem to be applicable as it results in less error chances. Furthermore, from the calculation of μ_v, as per the recommendation of ITU-R P.311-15, the proposed approach and the ITU-R P.530-16 and Moupfouma models show relatively lower values which are supported by lower σ_v and ρ_v which justified its suitability for the estimation of rain attenuation in terrestrial microwave links for lower frequency ranges.

Additionally, the calculated error matrix values obtained after the application of proposed approach for 38 and 75 GHz are depicted in Table 4(c). This show the lower values of relative error percentage for all interval of time percentage which is justified from decreased STD and RMS error. Furthermore, lower values of mean error are obtained as per the recommendation of ITU-R P.311-15 which is supported by lower values of σ_v and ρ_v.

5. Conclusion

In this paper, a comparison of rain attenuation at a lower microwave frequency particularly, 18 GHz, was made with the calculated rain attenuation distribution and four existing models for $0.001\% \leq P \leq 1\%$ of the time. The results of the three-year measurement of rain-induced attenuation and rain rate for a 1-minute interval from 2013 to 2015 for Icheon region are studied. The experimental results are observed to be underestimated by the ITU-R P.530-16 method for a path length of 3.2 km, and a similar pattern is observed from the da Silva Mello, Moupfouma, and Abdulrahman models. Interestingly, the da Silva Mello and Abdulrahman models can be used for higher time percentages when $0.5\% \leq P \leq 1\%$ of the time under horizontal and vertical polarization. Similarly, for lower time percentage when $0.001\% \leq P \leq 0.3\%$, these models generate higher relative error values and the proposed approach produces lower values. The suitability of the proposed approach is further tested in 38 and 75 GHz links. The proposed attenuation prediction approach presents the relationship between theoretical specific rain attenuation as specified by ITU-R P.838-3, $\gamma_{\%p}$, and effective specific rain attenuation, γ_{eff}. The relative error margin of 13%, 5%, 16% and 23%, 6%, 9% were obtained for 0.1%, 0.01%, and 0.001% of the time under 18 GHz for horizontal and vertical polarization, respectively. Similarly, for 38 and 75 GHz, the calculated relative error of 24%, 7%, 8% and 18%, 5%, 8% are acquired in similar time instances. Particularly, in 0.01% of the time, the measured result shows 32.57

and 21.88 dB, a difference of about 11 dB, for horizontal and vertical polarization as compared with the ITU-R P.530-16 prediction of 13.47 and 11.18 dB, respectively. Furthermore, the proposed method results in 31.07 and 23.09 dB for horizontal and vertical polarization, respectively. Unfortunately, the proposed approach is limited by the data sources of other regions for link operating in different terrains and longer hop lengths. The proposed model validity can only be established when it is tested over varying path lengths and range of frequencies and terrains in South Korea, or in the Korean Peninsula or North-East Asia. Under such circumstances, the ITU-R P.530-16 and Moupfouma models provide the reasonable estimation. Additionally, it is observed that for higher time percentages particularly, $0.5\% \leq P \leq 1\%$ of the time, the da Silva Mello Model and Abdulrahman model hold better estimation. Conversely, for lower time percentages, $0.001\% \leq P \leq 0.3\%$ of the time, ITU-R P.530-16 and Moupfouma models can be applied. Furthermore, it is observed that horizontal polarization is more prone to rain fades because as raindrops increase in size, they get more extended in the horizontal direction and therefore will attenuate horizontal polarization more than vertical polarization. Furthermore, the paper presents the rainfall rate derived from the Korea Meteorological Administration (KMA) and National Radio Research Agency (RRA).

Overall, it can be concluded that the proposed approach is suitable for one link where the measurements were performed that ensure link availability and reliable communication during rain events and quality of service for the end user. It should be noted that the results are valid for this particular climates, and its feasibility for other regions requires more testing and analyses.

Data Availability

The data type used to support the findings of this study have not been made available because of privacy issues of the measured data sets which could be made available from the National Radio Research Agency, RRA, upon request.

Conflicts of Interest

The authors declare that they have no competing interests.
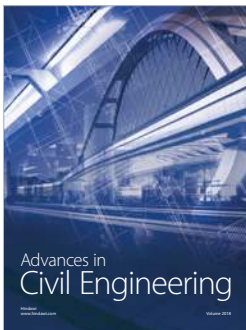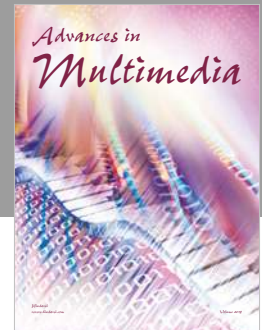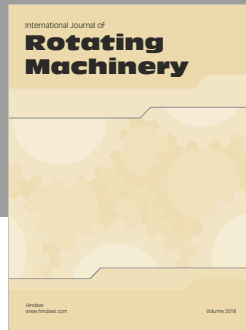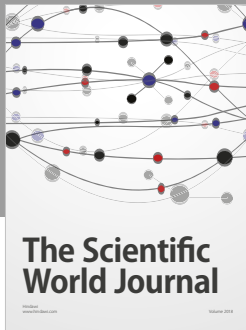
Acknowledgments

References

[1] R. K. Crane, *Electromagnetic Wave Propagation through Rain*, Wiley-Interscience, 1996.

[2] R. L. Freeman, *Radio System Design for Telecommunication*, John Wiley & Sons Inc, San Francisco, CA, USA, 3rd edition, 2007, A Wiley inter-science publication.

[3] S. Sujan, J.-J. Park, and D.-Y. Choi, "Rain rate modeling of 1-min from various integration times in South Korea," *Springerplus*, vol. 5, no. 1, p. 433, 2016.

[4] S. Sujan, P. Jung-Jin, S. W. Kim, J. J. Kim, J. H. Jung, and D. Y. Choi, "1-Minute rain rate derivation from various integration times in South Korea," in *Proceedings of the 1st International Conference on Next Generation Computing*, Bangkok, Thailand, January 2016.

[5] S. Sujan and D.-Y. Choi, "Proposed one-minute rain rate conversion method for microwave applications in Korea," *Journal of information and communication convergence engineering*, vol. 14, no. 3, pp. 153–162, 2016.

[6] R. M. D. Islam, Y. A. Abdulrahman, and T. A. Rahman, "An improved ITU-R rain attenuation prediction model over terrestrial microwave links in tropical region," *EURASIP Journal on Wireless Communications and Networking*, vol. 2012, no. 1, p. 189, 2012.

[7] I. T. U.-R. P. 530-16, "Propagation data and prediction methods required for the design of terrestrial line-of-sight systems," ITU, Geneva, Switzerland, 2015.

[8] L. A. R. da Silva Mello, M. S. Pontes, R. M. de Souza, and N. A. Pérez García, "Prediction of rain attenuation in terrestrial links using full rainfall rate distribution," *Electronics Letters*, vol. 43, no. 25, pp. 1442-1443, 2007.

[9] L. Mello and M. S. Pontes, "Unified method for the prediction of rain attenuation in satellite and terrestrial links," *Journal of Microwaves, Optoelectronics and Electromagnetic Applications*, vol. 11, no. 1, pp. 1–14, 2012.

[10] F. Moupfouma, "Electromagnetic waves attenuation due to rain: a prediction model for terrestrial or L.O.S SHF and EHF radio communication links," *Journal of Infrared, Millimeter, and Terahertz Waves*, vol. 30, no. 6, pp. 622–632, 2009.

[11] A. Y. Abdulrahman, T. A. Rahman, S. K. A. Rahim, and M. R. U. Islam, "Empirically derived path reduction factor for terrestrial microwave links operating at 15 GHz in Peninsula Malaysia," *Journal of Electromagnetic Waves and Applications*, vol. 25, no. 1, pp. 23–37, 2011.

[12] Y. A. IO, B. Olusegun, and N. H. H. Khamis, "Comparative analysis of terrestrial rain attenuation at Ku band for stations in South-Western Nigeria," *International Research Journal of Engineering and Technology*, vol. 3, pp. 27–35, 2016.

[13] K. Ulaganathen, A. R. Tharek, R. M. Islam, and K. Abdullah, *Case Study of Rain Attenuation At 26 GHz in Tropical Region (Malaysia) for Terrestrial Link*.

[14] J. S. Mandeep, "Rain attenuation statistics over a terrestrial link at 32.6 GHz at Malaysia," *IET Microwaves, Antennas & Propagation*, vol. 3, no. 7, pp. 1086–1093, 2009.

[15] U. Kesavan, T. A. Rahman, A. Y. Abdulrahman, and S. K. B. A. Rahim, "Comparative studies of the rain attenuation predictions for tropical regions," *Progress In Electromagnetics Research*, vol. 18, pp. 17–30, 2011.

[16] S. Shrestha and D.-Y. Choi, "Study of 1-min rain rate integration statistic in South Korea," *Journal of Atmospheric and Solar-Terrestrial Physics*, vol. 155, pp. 1–11, 2017.

[17] S. Shrestha and D.-Y. Choi, "Characterization of rain specific attenuation and frequency scaling method for satellite communication in South Korea," *International Journal of Antennas and Propagation*, vol. 2017, Article ID 8694748, 16 pages, 2017.

[18] S. Shrestha and D.-Y. Choi, "Diurnal and monthly variations of rain rate and rain attenuation on Ka-band satellite communication in South Korea," *Progress In Electromagnetics Research*, vol. 80, pp. 151–171, 2018.

[19] S. Sujan, I. Nadeem, K. Sun-Woong, H. Seung-Jo, and D. Y. Choi, "Rain specific attenuation and frequency scaling approach in slant-path for Ku and Ka-band experiments in South Korea," in *ICEIC 2017 International Conference on Electronics, Information, and Communication*, pp. 625–628, Phuket, Thailand, January 2017.

[20] A. Y. Abdulrahman, T. A. Rahman, S. K. A. Rahim, M. R. Islam, and M. K. A. Abdulrahman, "Rain attenuation predictions on terrestrial radio links: differential equations approach," *European Transactions on Telecommunications*, vol. 23, no. 3, pp. 293–301, 2012.

[21] V. Kvicera and M. Grabner, "Rain attenuation at 58 GHz: prediction versus long-term trial results," *EURASIP Journal on Wireless Communications and Networking*, vol. 2007, no. 1, article 046083, 2007.

[22] G. Rakshit, A. Adhikari, and A. Maitra, "Modelling of rain decay parameter for attenuation estimation at a tropical location," *Advances in Space Research*, vol. 59, no. 12, pp. 2901–2908, 2017.

[23] ITU-R, *Specific Attenuation Model for Rain for Use in Prediction Methods, Recommendation P.838-3*, ITU-R Recommendations, P Series, International Telecommunications Union, Geneva, 2005.

[24] "National Radio Research Agency (RRA) 767, Bitgaram-ro, Naju-si, Jeollanam-do 58217, Republic of Korea," http://www.rra.go.kr/en/index.jsp.

[25] OTT, *Operating instructions: Present Weather Sensor Parsivel*, 70.200.005.B.E 08-1008, https://www.ott.com/download/operating-instructions-present-weather-sensor-ott-parsivel2-without-screen-heating/.

[26] S. Shrestha and D.-Y. Choi, "Rain attenuation over terrestrial microwave links in South Korea," *IET Microwaves, Antennas & Propagation*, vol. 11, no. 7, article 1031, 2017.

[27] S. Sujan and D.-Y. Choi, "Study of rain attenuation in Ka band for satellite communication in South Korea," *Journal of Atmospheric and Solar-Terrestrial Physics*, vol. 148, pp. 53–63, 2016.

[28] D. Y. Choi, J. Y. Pyun, S. K. Noh, and S. W. Lee, "Comparison of measured rain attenuation in the 12.25-GHz band with predictions by the ITU-R model," *International Journal of Antennas and Propagation*, vol. 2012, Article ID 415398, 5 pages, 2012.

[29] ITU-R P311-15, *Acquisition, Presentation and Analysis of Data in Studies of Radio Wave Propagation*, International Telecommunication Union, Geneva, 2015.

[30] R. K. Crane, "A local model for the prediction of rain-rate statistics for rain-attenuation models," *IEEE Transactions on Antennas and Propagation*, vol. 51, no. 9, pp. 2260–2273, 2003.

[31] A. P. Bonati, "Essential knowledge of rain structure for radio application based on available data and models," *Radio Africa*, vol. 99, 1999.

[32] F. Davarian, *Proceedings of the Seventeenth NASA Propagation Experimenters Meeting (NAPEX 17) and the Advanced Communications Technology Satellite (ACTS) Propagation Studies Miniworkshop*, NASA United States, 1993.

[33] U. Kesavan, A. R. Tharek, and M. R. Islam, "Comparison of microwave path lengths between temperate and tropical region based on effects of rain," in *PIERS Proceedings*, Moscow, Russia, August, 2012.

[34] *The Mathworks, Inc. Protected by U.S. and International Patents*, http://www.mathworks.com.

[35] S. Sujan and D.-Y. Choi, "Rain attenuation statistics over millimeter wave bands in South Korea," *Journal of Atmospheric and Solar-Terrestrial Physics*, vol. 152-153, pp. 1–10, 2016.

[36] M. C. Kestwal, S. Joshi, and L. S. Garia, "Prediction of rain attenuation and impact of rain in wave propagation at microwave frequency for tropical region (Uttarakhand, India)," *International Journal of Microwave Science and Technology*, vol. 2014, Article ID 958498, 6 pages, 2014.

[37] ITU-R P837-6, *Characteristics of Precipitation for Propagation Modeling*, International Telecommunication Union, Geneva, 2012.